



# Mechanisms and kinetics of electrode processes at bismuth and antimony film and bare glassy carbon surfaces under square-wave anodic stripping voltammetry conditions

Valentin Mirceski <sup>a,b,\*</sup>, Bine Sebez <sup>c</sup>, Maja Jancovska <sup>b</sup>, Bozidar Ogorevc <sup>c</sup>, Samo B. Hocevar <sup>c</sup>

<sup>a</sup> Institute of Chemistry, Faculty of Natural Sciences and Mathematics, "Ss Cyril and Methodius" University, P.O. Box 162, 1000 Skopje, Republic of Macedonia

<sup>b</sup> Medical Faculty, University "Goce Delčev", P.O. Box 201, 2000 Štip, Republic of Macedonia

<sup>c</sup> Analytical Chemistry Laboratory, National Institute of Chemistry, Hajdrihova 19, SI-1000 Ljubljana, Slovenia



## ARTICLE INFO

### Article history:

Received 2 February 2013

Received in revised form 15 April 2013

Accepted 20 April 2013

Available online 7 May 2013

### Keywords:

Anodic striping voltammetry  
Square-wave voltammetry  
Electrode mechanisms  
Electrode kinetics

## ABSTRACT

Mechanism and kinetics of anodic stripping electrode processes of Zn(II), Cd(II) and Pb(II) at bismuth (BiFE) and antimony (SbFE) film as well as bare glassy carbon (GCE) electrodes have been studied with respect to our recent published theoretical considerations developed for square-wave voltammetry (SWV). Mechanistic aspects of electrode reactions have been elucidated by a qualitative comparison of simulated and experimental data for three different electrode reaction mechanisms, i.e. simple anodic stripping mechanism, anodic stripping mechanism coupled with adsorption of metal analyte ions, and mechanism affected by interactions within the particles of the metal deposit on the electrode surface. The electrode kinetics has been estimated by the method of quasireversible maximum and by analyzing the peak potential separation between forward and backward SW components, under variation of the SW amplitude. Electrode mechanisms and kinetics are different at bismuth compared to antimony film electrodes. The electrode reactions of Pb(II) and Cd(II) at BiFE involve adsorption phenomena, while electrode processes of all three analytes are free of adsorption at SbFE. At BiFE, the electron transfer standard rate constants of all three analytes are quite comparable, ranging within the interval from 1 to  $3 \text{ cm s}^{-1}$ . At SbFE the electrode kinetics of Cd(II) and Pb(II) are almost the same, while the electrode reaction of Zn(II) is significantly slower. Our results showed that the kinetics of all examined electrode reactions are slower at SbFE as compared to those observed at BiFE.

© 2013 Elsevier Ltd. All rights reserved.

## 1. Introduction

Electrochemical techniques have been proven to be versatile tools for trace metal determination. Among them, stripping voltammetry is particularly powerful method due to effective pre-concentration of the analyte prior to the detection (stripping) step, thus being attributed with a remarkable sensitivity and associated low detection limits [1]. Performance of a stripping voltammetric procedure depends primarily on the appropriate choice of the working electrode. Hence, the electrode material, its surface morphology, as well as the knowledge of the electrode mechanisms, are among the critical factors determining the analytical performance.

Different substrates, most frequently a variety of carbon materials and metals, have been employed for the fabrication of working electrodes. In particular, glassy carbon electrode (GCE) has gained wide acceptance due to its convenient electrical/electroanalytical and mechanical properties and the ease of operation. During the last four decades glassy carbon electrodes have been extensively utilized, either as a bare electrode, or being a subject of a surface modification [2–4]. Mercury film electrode (MFE), typically prepared by using GCE as a substrate, has been traditionally used in voltammetric and potentiometric stripping analysis of metal ions, because of its extremely favourable signal-to-background ratio and overall electroanalytical performance [5,6]. However, mercury related electrodes are associated with well-known drawbacks concerning toxicity, handling and disposal of mercury. Fortunately, a bit more than a decade ago, a novel bismuth film electrode (BiFE) was developed as a convenient alternative to the MFE [7]. This pioneering work provoked a plethora of studies focused on non-mercury film electrodes for trace metal analysis. In order to find the most suitable and desired analytical performance, different

\* Corresponding author at: Institute of Chemistry, Faculty of Natural Sciences and Mathematics, "Ss Cyril and Methodius" University, P.O. Box 162, 1000 Skopje, Republic of Macedonia. Tel.: +389 71219828; fax: +389 23226865.

E-mail address: [valentin@pmf.ukim.mk](mailto:valentin@pmf.ukim.mk) (V. Mirceski).

configurations of bismuth electrodes have been employed for measuring metal ions [8–12] as well as miscellaneous organic compounds relevant to the environment, medicine, etc. [13,14]. Subsequently, another novel metal film electrode, the antimony film electrode (SbFE) was also introduced a few years ago [15]. Similar to their bismuth analogue, the antimony based electrodes are attributed with acceptable characteristics for electroanalytical (stripping) analysis such as an auspicious performance in more acidic media, a favourably negative potential for hydrogen evolution process, and unexpectedly low stripping signal of the antimony itself [16–22].

While the overall analytical performance of BiFEs and SbFEs has been already thoroughly examined, systematic mechanistic and kinetic studies at these electrodes are still missing. Recently, an attempt was made to develop a phenomenological theoretical background to rationalize some of possible electrode mechanisms [23] under conditions of square-wave voltammetry (SWV) [24,25]. In the present communication we apply the recent theory [23] to characterize the anodic stripping electrode mechanisms of Pb(II), Cd(II) and Zn(II) from mechanistic and kinetic point at both BiFEs and SbFEs, while the mechanism of Pb(II) was studied at bare GCE as well.

## 2. Experimental

### 2.1. Apparatus

Anodic stripping voltammetric (ASV) measurements were performed with the modular electrochemical workstation (Autolab, Eco Chemie, Utrecht, The Netherlands) equipped with PGSTAT12 driven by GPES software (Eco Chemie). A three-electrode configuration was used, consisting of a bismuth or antimony film modified or a bare glassy carbon disc electrode ( $d = 2$  mm), Ag/AgCl (KCl 3 M), and a platinum wire as the working, reference, and counter electrode, respectively. All electrochemical experiments were carried out in a 20 mL one-compartment voltammetric cell at conditioned room temperature ( $23 \pm 1^\circ\text{C}$ ).

### 2.2. Reagents

Standard stock solutions of bismuth(III), antimony(III), cadmium(II), lead(II), and zinc(II) ( $1 \text{ g L}^{-1}$ , atomic absorption standard solution) were obtained from Aldrich and diluted as required. A 0.1 M sodium acetate buffer solution (pH 4.5) served as the supporting electrolyte for experiments with BiFEs, while 0.01 M  $\text{HNO}_3$  solution was the supporting electrolyte for experiments with SbFEs. Water used to prepare all solutions was first deionized and then further purified via an Elix 10/Milli-Q Gradient unit (Millipore, Bedford, MA).

### 2.3. Procedures

ASV measurements were performed by the *in situ* accumulation of bismuth or antimony film together with target metal ions in the presence of dissolved oxygen. Prior to its use, the glassy carbon disc electrode was polished with a  $0.05 \mu\text{m}$  alumina slurry on a polishing pad and rinsed with water. The polished working electrode was immersed into a 20 mL electrochemical cell containing either 0.1 M acetate buffer solution and  $20 \mu\text{M}$  of Bi(III) ions (for studies at *in situ* BiFEs), or 0.01 M  $\text{HNO}_3$  solution containing  $20 \mu\text{M}$  of Sb(III) ions (for studies at *in situ* SbFEs).

At BiFEs the accumulation potential of  $-1.4 \text{ V}$  was applied without stirring, in order to obtain the metal deposit morphology as uniform as possible, being in accordance with the theoretical assumptions upon which the theoretical model is based [23]. The anodic stripping voltammogram was recorded by applying a

positive-going square-wave potential scan with a potential step of usually 2 mV and with a frequency and an amplitude as denoted in each experiment. Aliquots of the target metal ion standard solution were introduced after recording the background stripping voltammogram. Prior to the next cycle, a 30 s conditioning step at  $+0.3 \text{ V}$  under stirring conditions was used to remove completely the accumulated metals and bismuth film.

For experiments with Pb(II) at bare GCE, the same procedure has been followed as for BiFEs, only the supporting electrolyte was free of Bi(III) ions.

A similar procedure was applied at SbFEs, composed of an electrochemical accumulation step at  $-1.3 \text{ V}$  for a period of 120 s without stirring, which was followed by a square-wave voltammetric scan from  $-1.3 \text{ V}$  to  $+0.3 \text{ V}$ . Prior to each ASV measurement, the cleaning step was applied by holding the working electrode at the potential of  $+0.3 \text{ V}$  for 20 s, while stirring the solution.

## 3. Results and discussion

### 3.1. Theoretical considerations

The recent theoretical treatment of anodic stripping voltammetric processes at BiFEs [23] under conditions of SWV encompassed three different mechanisms: (i) *simple anodic stripping mechanism* in which the metal analyte ions are the subject of diffusion mass transport following the stripping step, (ii) *adsorption mechanism*, in which the diffusion mass transport is coupled with a partial adsorption of the analyte ions on the Bi-film surface, and (iii) *adsorption-interaction mechanism* in which, besides adsorption and diffusion, the role of interactions (attractive or repulsive) between accumulated metal particles have been taken into account. The latter mechanism is the most general one, providing a basis for detail qualitative description of the majority of the experimental data. The previous two simpler mechanisms could be considered as limiting cases of adsorption-interaction mechanism. More specifically, if the degree of interactions is insignificant the adsorption-interaction mechanism simplifies to the adsorption mechanism and further, if the adsorption is insignificant, the system eventually converges to the simple anodic stripping mechanism.

The stripping voltammetric features of the adsorption-interaction mechanisms are predominantly controlled by the interaction parameter  $\zeta = a\sqrt{D/f}(c_M^*/\Gamma_{\max})$ , where  $a$  is Frumkin interaction parameter,  $D$  is diffusion coefficient of the metal analyte ion,  $f$  is frequency of the SW potential modulation,  $c_M^*$  is bulk concentration of the metal analyte, and  $\Gamma_{\max}$  is maximal surface concentration of the metal deposit on the electrode substrate. Indeed, the degree of interactions depends mainly on the Frumkin interaction parameter, as a typical dimensionless constant for a given experimental system with  $a < 0$  and  $a > 0$  for repulsive and attractive interactions, respectively, and the fractional coverage of the electrode surface with accumulated metal particles. In addition, all parameters controlling the surface coverage, i.e. the analyte concentration, time and potential of the accumulation, diffusion coefficient, and the SW frequency, further affect the degree of interactions. The presence and type of interactions can be determined by a simple analysis of the net anodic SW voltammetric peak potential ( $E_p$ ) variation with the accumulation time and/or concentration of the analyte. When attractive or repulsive forces are operative the peak potential shifts towards less or more negative potentials, respectively, which can be easily examined by increasing either or both metal analyte concentration or deposition time. Another diagnostic criterion can be based on the evolution of the quasireversible maximum (QRM) as a function of the concentration or accumulation time. In Fig. 1 it is clearly shown that the position of the QRM is affected by the analyte concentration in the presence of interactions, which is not the case for the system free of interactions. The

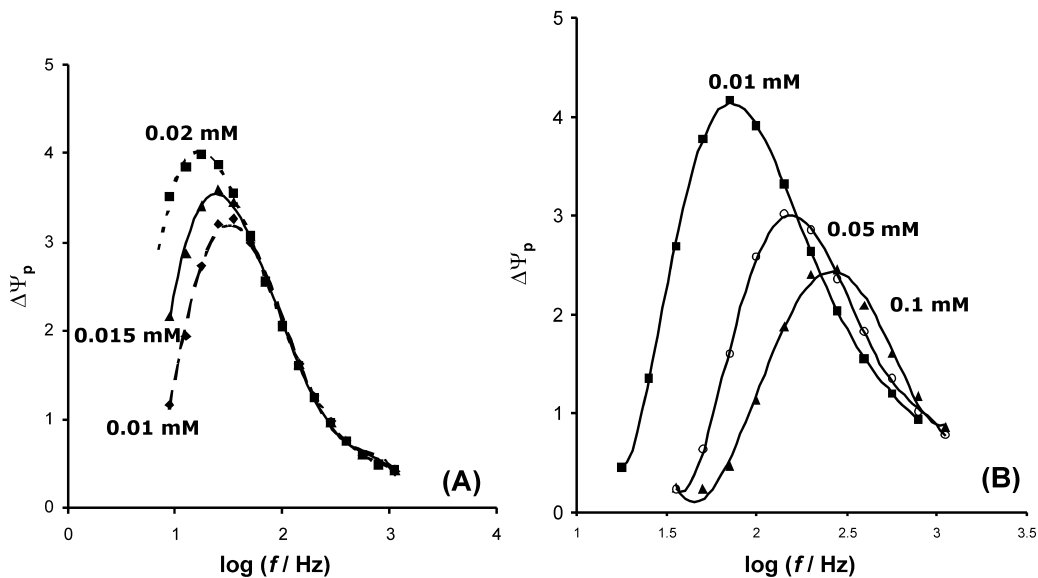


**Fig. 1.** Theoretical data obtained with the simulation of the adsorption-interaction anodic stripping mechanism [23]. The effect of metal analyte concentration on the position of the quasireversible maximum in the case of attractive (A) and repulsive forces (B). The Frumkin interaction parameter is  $a = 1$  (A) and  $-2.5$  (B). Other conditions of the simulations are: standard rate constant  $k_s = 50 \text{ s}^{-1}$ , electron transfer coefficient  $\alpha = 0.5$ , adsorption constant  $\beta = 0.1 \text{ cm}$ , number of exchanged electrons  $n = 1$ , maximal surface concentration  $I_{\max} = 10^{-10} \text{ mol/cm}^2$ , step potential  $\Delta E = 5 \text{ mV}$ , and SW amplitude  $E_{\text{sw}} = 25 \text{ mV}$  (A) and  $50 \text{ mV}$  (B). The ordinate displays the dimensionless net SW peak current  $\Delta\Psi_p$  [23].

increase of concentration shifts the QRM in a direction depending on the type of interactions (compare panels A and B in Fig. 1). More specifically, for repulsive forces the QRM shifts towards higher critical frequencies, whereas the shift is opposite for attractive forces. We recall that the QRM is a parabolic dependence of the dimensionless net peak current  $\Delta\Psi_p$  (or frequency normalized real net peak current,  $\Delta I_p f^{-0.5}$ ) on the logarithm of the frequency; its origin, physical meaning, and application for kinetic measurements have been elaborated in detail in previous studies [24,25].

Although the adsorption-interaction mechanism is the most general one, enabling qualitative characterization of the experimental system in detail, it is very complex and dependent on a number of parameters [23]. Quantitative comparison with experimental data for the purpose of unambiguous estimation of the electrode kinetics parameters (i.e. the electron transfer standard rate constant,  $k_s$ ) is thus precluded. For these reasons, it is highly recommended to simplify the experimental system and to assimilate the stripping voltammetric behaviour to the simpler mechanism, preferably to the *simple anodic stripping mechanism*.

For the purpose of kinetic measurements, besides the application of the QRM which requires variation of the SW frequency, one can take advantage of using SW amplitude, as a second powerful instrumental tool for interrogation of the experimental system. As already demonstrated [26,27], the SW amplitude is particularly useful for analysis of surface confined electrode mechanisms. In this methodology, the peak potential separation between the forward (anodic) and backward (cathodic) SW stripping voltammetric components is analyzed as a function of the SW amplitude, for a given frequency. Unfortunately, this method is ineffective for the simple anodic stripping mechanism. To circumvent this drawback, we proposed a simple modification in the presentation of the SW stripping voltammetric data. Namely, the SW potential modulation consists of a staircase potential ramp, upon which potential pulses of a given height (i.e.  $E_{\text{sw}}$  amplitude) are superimposed. The current is measured at the potential of the pulse, but plotted versus the potential of the staircase ramp [24,25]. Presenting the data in this way is justified from an analytical point of view, but has some drawbacks in the context of electrode kinetic measurements. The detailed discussion of this issue will be provided

in our next publication. Hence, we propose the construction of a potential-corrected SW stripping voltammogram (avoiding the net SW component), in which the forward and backward SW components are presented versus the potential of the pulses, i.e. versus the real potentials of measurements. The effect of this correction is illustrated in Fig. 2. The forward and backward SW components of the original stripping voltammogram (A) are shifted towards more positive and more negative potentials of the potential-corrected stripping voltammogram (B), respectively, for the value of the used amplitude. Fig. 3 shows that the potential separation of the components of the potential-corrected stripping voltammogram is a linear function of the SW amplitude (curve 2), which is not the case for the original stripping voltammogram (curve 1), considering simple anodic stripping mechanism. The slope and intercept are sensitive to the standard rate constant, thus enabling electrode kinetic measurements. This methodology enables electrode kinetic measurements at a constant frequency, i.e. at a constant scan rate, which has obvious advantages.

### 3.2. Experimental results

In the majority of our anodic stripping voltammetric experiments with Zn(II), Cd(II) and Pb(II) at BiFE, in which the bismuth film was *in situ* deposited, the net SW peak potentials were sensitive to the analyte concentration and accumulation time. This is also true for most of the literature data [28]. Interestingly, the peak potential of Zn(II) shifts towards more negative potentials by increasing its concentration, whereas the opposite shift was observed for Cd(II) and Pb(II). Over the concentration interval from 1 to  $5 \mu\text{M}$  of Zn(II) and accumulation time of 120 s, the dependence  $E_p$  vs.  $\log c(\text{Zn}^{2+})$  is linear with a slope of  $-68 \text{ mV}$  ( $R = 0.988$ ). The same phenomena can be reproduced with the adsorption-interaction model assuming repulsive interactions (i.e. the Frumkin interaction parameter  $a \approx -2.5$ ). The quasireversible maximum of Zn(II) shifts towards higher frequencies by increasing either concentration of Zn(II) ions or accumulation time. For instance, the critical frequencies associated with the position of the maximum are  $f_{\max} = 240$  and  $320 \text{ Hz}$ , for accumulation times of 180 and 240 s, respectively. These experimental data are in

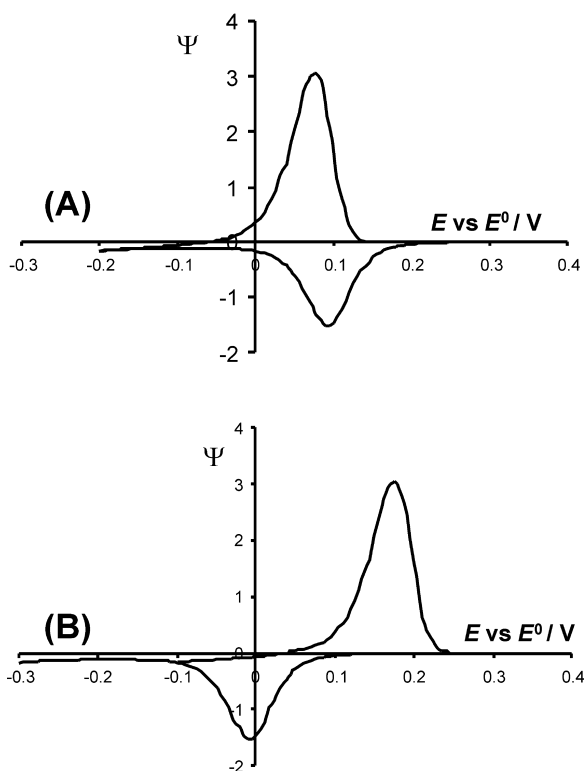


**Fig. 2.** Theoretical data obtained with the simulation of the simple anodic stripping mechanism [23]. Original (A) and potential corrected SW voltammogram (B) simulated for SW amplitude of  $E_{\text{sw}} = 100 \text{ mV}$ . The other conditions of the simulations are: standard rate constant  $k_s = 0.01 \text{ cm s}^{-1}$ , electron transfer coefficient  $\alpha = 0.5$ , number of exchanged electrons  $n = 2$ , SW frequency  $f = 10 \text{ Hz}$ , and step potential  $\Delta E = 5 \text{ mV}$ .

accordance with theoretical prediction illustrated in Fig. 1B, confirming the repulsive forces between the accumulated zinc metal particles. Yet, the physical origin of this phenomenon remains to be revealed.

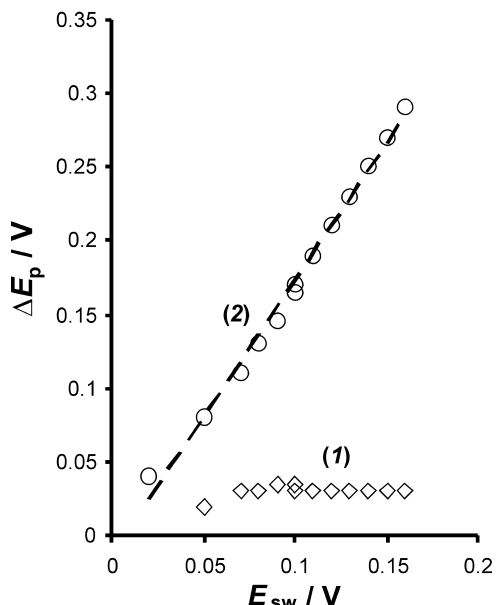


**Fig. 3.** Theoretical data obtained with the simulation of the simple anodic stripping mechanism [23]. The dependence of the peak potential separation between forward (anodic) and backward (cathodic) components of the SW voltammetric response on the SW amplitude for the original (1) and potential corrected (2) SW voltammograms of a simple anodic stripping mechanism with the standard rate constant of  $k_s = 0.1 \text{ cm s}^{-1}$ . The other conditions of the simulations are the same for Fig. 2.

Although electrode mechanisms are in a qualitative agreement with the adsorption-interaction model, for electrokinetic measurements it is recommended to simplify the experimental system in order to permit application of the simple anodic stripping reaction model. Taking into account the definition of the interaction parameter (Section 3.1), it is obvious that the degree of interactions can be minimized by decreasing the analyte concentration and/or by increasing the frequency of the potential modulation. Hence, experimental results obtained with a low analyte concentration ( $\leq 2 \mu\text{M}$ ) and relatively high frequency ( $\geq 150 \text{ Hz}$ ) meet these criteria and can be processed according to the model of the simple anodic stripping mechanism. Thus, the standard rate constant can be estimated either by inspecting the potential separation between the forward and backward SW components as a function of the SW amplitude, or by applying the methodology of the quasireversible maximum. Fig. 4A shows the best fit between the experimental and theoretical data for the potential separation by changing the SW amplitude, considering potential corrected SW voltammograms of Zn(II). As the effect of interactions is assumed to be insignificant, the simulated data refer to the simple anodic stripping model. The best fit between the experimental and theoretical data was found for the standard rate constant  $k_s = 1 \text{ cm s}^{-1}$ , assuming  $\alpha = 0.5$  ( $\alpha$  is the electron transfer coefficient). The correlation between experimental and theoretical data resulted in a line with a slope of 1.05 and regression coefficient  $R = 0.999$ , reflecting the quality of fitting. By applying the second method for estimation of the standard rate constant based on the QRM (Fig. 4B), the value of  $k_s = 3 \text{ cm s}^{-1}$  was obtained, which is in accord with the previous one.

Anodic stripping voltammetric patterns of Cd(II) and Pb(II) are significantly different compared to Zn(II). As shown in Fig. 5A, the increasing of the accumulation time causes the responses of both Cd(II) and Pb(II) to shift in a positive potential direction. The same effect can be achieved by increasing the concentration of metal analyte ions at a constant accumulation time. In addition, as shown in Fig. 5B, the QRM of Pb(II) shifts towards lower critical frequencies by increasing the concentration, confirming the attractive forces between the accumulated metal particles. In addition to the attractive forces, the electrode mechanisms of both Cd(II) and Pb(II) are coupled by partial adsorption of the metal ions [23]. This assumption is supported by the linear dependence of the peak current of the backward (reductive) SW component on the frequency over the interval from 8 to 100 Hz, for both Cd(II) and Pb(II) with a linear regression coefficient  $R = 0.997$  and 0.998, respectively. However, splitting of the net SW voltammetric peak was not observed under large SW amplitude, as predicted by the adsorption mechanism. This implies that the adsorption of Cd(II) and Pb(II) is weak, causing their electrode mechanisms to be of a mixed nature, involving electrode reactions from both adsorbed and dissolved state of the analyte. Applying the QRM at low concentrations of the metal analyte ions, (e.g.  $2 \mu\text{M}$ ) in order to diminish the effect of interactions and to model the experimental system with the simple anodic stripping mechanism, the obtained critical frequencies are close to those of Zn(II) ( $f_{\text{max}}(\text{Zn}) = 420 \text{ Hz}$ ,  $f_{\text{max}}(\text{Cd}) = 480 \text{ Hz}$ , and  $f_{\text{max}}(\text{Pb}) = 370 \text{ Hz}$ ). Hence, the standard rate constants of all three analytes estimated by using QRM fall in the interval of  $1\text{--}3 \text{ cm s}^{-1}$ , revealing very fast electrode processes.

Performing anodic stripping voltammetric measurements of Pb(II) at bare GCE, significantly different voltammetric patterns have been observed compared to BiFEs. Fig. 6 compares typical SW voltammetric responses (net component is not shown) at the two different electrode substrates. At BiFE (B), the relative position of the forward (anodic) and backward (cathodic) components is in accordance with the prediction of the simple anodic stripping model assuming an electron transfer coefficient  $\alpha = 0.5$ , i.e. the forward component is positioned at more negative potentials relative to the backward one. However, at bare GCE the relative

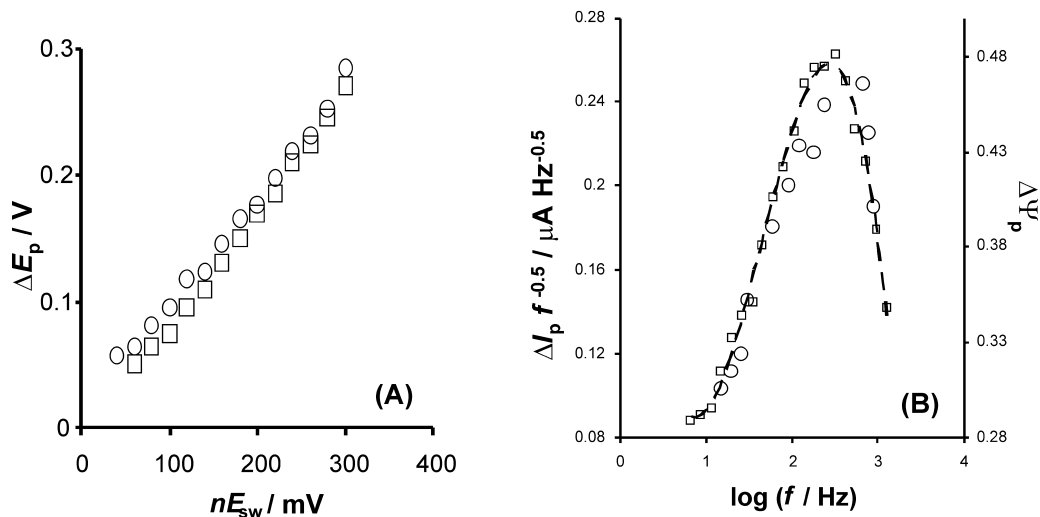


**Fig. 4.** Anodic stripping voltammetry of Zn(II) at BiFE. (A) The best fit between the experimental (circles) and theoretical (squares) data for the forward and backward peak potential separation as a function of the SW amplitude of the potential-corrected SW voltammograms, measured at frequency of  $f = 150$  Hz. The theoretical data correspond to the simple anodic stripping mechanism with the standard rate constant of  $k_s = 1 \text{ cm s}^{-1}$  and electron transfer coefficient  $\alpha = 0.5$ . Experimental conditions are:  $c(\text{Zn}^{2+}) = 2 \mu\text{M}$ , accumulation time  $t_{\text{acc}} = 120$  s (without stirring) and accumulation potential  $E_{\text{acc}} = -1.4$  V. (B) The best fit between the experimental (circles, left ordinate) and theoretical (squares, right ordinate) quasireversible maximum obtained for the standard rate constant of  $k_s = 3 \text{ cm s}^{-1}$  and SW amplitude of  $E_{\text{sw}} = 25$  mV. The other conditions are the same as for panel (A).

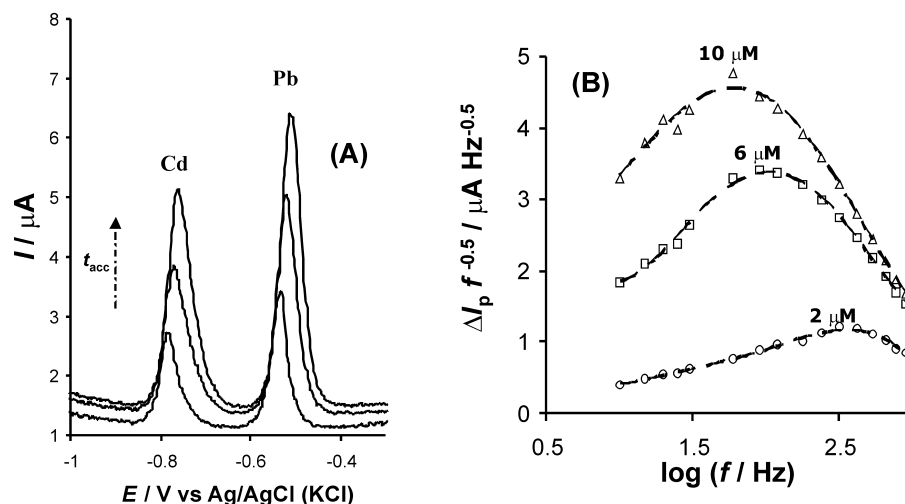


**Fig. 5.** (A) Typical evolution of anodic stripping net SW voltammograms of Cd(II) and Pb(II) by increasing the accumulation time from 20, 200 to 320 s. The experimental conditions are:  $c(\text{Cd}^{2+}) = c(\text{Pb}^{2+}) = 2 \mu\text{M}$ , frequency  $f = 25$  Hz, amplitude  $E_{\text{sw}} = 25$  mV, and step potential  $\Delta E = 2$  mV. The accumulation time values are given in the graph. (B) The evolution of the quasireversible maximum of Pb(II) by increasing the concentration of the metal analyte ions. Accumulation time is 120 s. The other conditions are the same as for (A).

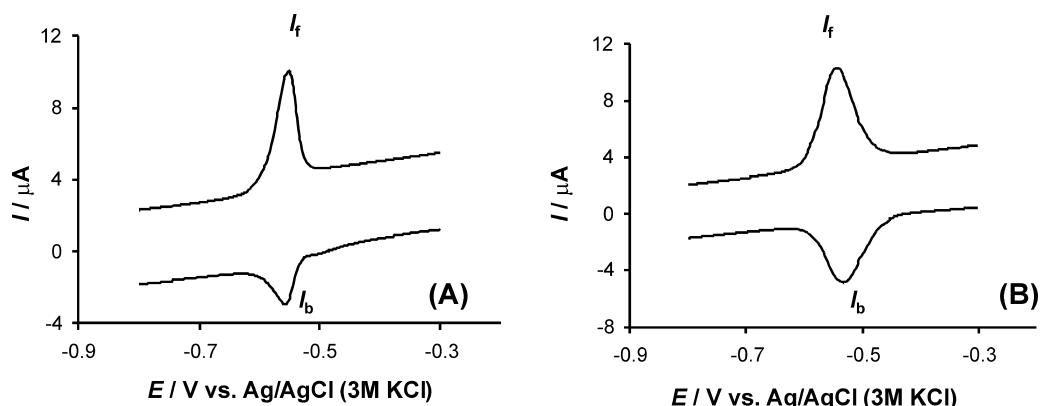


**Fig. 6.** Forward ( $I_f$ , anodic) and backward ( $I_b$ , cathodic) components of the SW voltammetric response of Pb(II) at a bare glassy carbon electrode (A) and BiFE (B), at frequency of  $f = 90$  Hz, amplitude  $E_{\text{sw}} = 50$  mV, and step potential of 2 mV. The other conditions are the same as for Fig. 5.

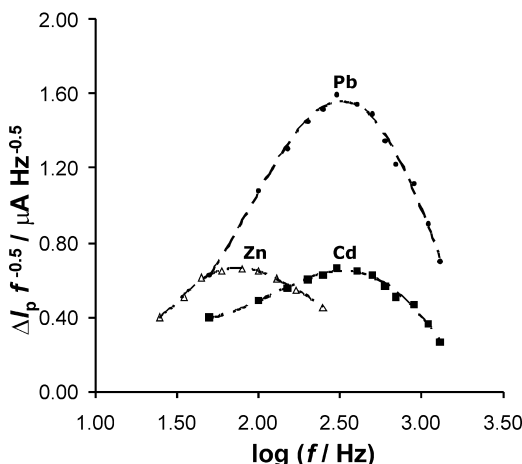


**Fig. 7.** Quasireversible maximum of 2 μM Zn(II), Cd(II) and Pb(II) at SbFEs recorded in 0.01 M HNO<sub>3</sub>. The other experimental conditions are: accumulation time  $t_{acc} = 120$  s (without stirring), accumulation potential  $E_{acc} = -1.3$  V, amplitude  $A_{sw} = 50$  mV, and step potential  $\Delta E = 2$  mV.

position of components is inverted (Fig. 6A). This phenomenon can be reproduced with the simple anodic stripping mechanism assuming  $\alpha > 0.5$  and  $k_s < 1 \text{ cm s}^{-1}$  revealing significant differences in the morphology of the accumulated metal and the rate of electron exchange. Moreover, the backward component at GCE is a linear function of the square-root of the frequency, implying that the mechanism is diffusion controlled, without adsorption of Pb(II) ions. In addition, the QRM at GC electrode is shifted towards less critical frequencies ( $f_{max} = 170$  Hz) compared to BiFE ( $f_{max} = 370$  Hz) confirming that the standard rate constant at the bare GCE is  $k_s < 1 \text{ cm s}^{-1}$ .

Finally, a brief analysis carried out of electrode mechanisms at SbFEs revealed significant differences in the kinetics and mechanisms of electrode reactions compared to BiFEs. It is important to stress that electrode mechanisms of all three analytes at SbFEs are free of adsorption phenomena. As depicted in Fig. 7, the critical frequency of the QRM measured at a low analyte concentration (i.e. 2 μM), is 80 Hz for Zn(II), and ca. about 300 Hz for both Cd(II) and Pb(II). Thus, the electrode kinetics of Cd(II) and Pb(II) are quite comparable, whereas the electrode reaction rate of Zn(II) is significantly slower. Furthermore, as concluded from the observed shifts of the net SW peak potentials with the accumulation time and concentration of metal analytes, all electrode mechanisms are affected by attractive interactions. For instance, by increasing the accumulation time from 300 s to 600 s the peak potentials shifted towards less negative potentials for 37, 45, and 70 mV for Cd(II), Pb(II), and Zn(II), respectively. This is in accord with the shift of the QRM by increasing the concentration of the analyte. For Zn(II), critical frequencies are 80, 55 and 35 Hz, for Zn(II) concentrations of 2, 6 and 10 μM, respectively, whereas, for both Pb(II) and Cd(II), the critical frequencies measured at these concentrations are 300, 200 and 120 Hz.

#### 4. Conclusions

It has been demonstrated that anodic stripping processes of Zn(II), Cd(II) and Pb(II) at BiFE and SbFE can be effectively studied in the light of the recent theory [23] developed for anodic stripping SWV. Mechanisms and kinetics of the three analytes are different and depend significantly on the electrode substrate. The anodic stripping of the metal deposit is frequently affected by the attractive forces acting between the deposited metal particles, although repulsive interactions have been also detected in the case of Zn(II) at the BiFE. The type and intensity of the interactions can

be evaluated by analysing the net peak potential shift as well as the shift of the QRM with analyte concentration and/or accumulation time. The formation of intermetallic compounds between different metal analytes that are simultaneously determined might be one of the reasons for the presence of interactions, although the physical origin of this phenomenon remains to be uncovered by means of experimental techniques different than voltammetry. The adsorption of analyte ions depends on both the type of electrode substrate and the nature of the analyte ions. Specifically, the electrode mechanisms of Cd(II) and Pb(II) at BiFE are partially affected by adsorption, whereas in all other cases adsorption is insignificant.

Kinetics of electrode reactions can be effectively estimated by means of QRM as well as by a novel approach based on the peak potential separation between the forward and backward components of the potential-corrected SW voltammograms. In the former method, one requires variation of the SW frequency, whereas in the latter, only variation of the potential modulation amplitude is required and the kinetic measurements are conducted at a constant scan rate of the voltammetric experiment, which is particularly advantageous. Generally speaking, the electrode reactions at BiFE are faster than at SbFE. The kinetics of all studied analytes is rather fast and comparable at BiFE, whereas at SbFE the kinetics of Zn(II) is significantly slower compared to Cd(II) and Pb(II).

#### Acknowledgements

Authors gratefully acknowledge the support of Ministries of Sciences of Macedonia and Slovenia through the bilateral cooperation program. VM acknowledges Alexander von Humboldt foundation for the financial support from the Research Group Linkage Programme 3.4-Fokop-DEU/1128670, as well as the support of DAAD foundation through multilateral project "International Masters and Postgraduate Programme in Materials Science and Catalysis" (Mat-CatNet).

#### References

- [1] J. Wang, Analytical Electrochemistry, third ed, Wiley-VCH, Hoboken, NJ, 2006.
- [2] R.C. Engstrom, V.A. Strasser, Characterization of electrochemically pretreated glassy carbon electrodes, *Analytical Chemistry* 56 (1984) 136.
- [3] A. Dekanski, J. Stevanovic, R. Stevanovic, B.Z. Nikolic, V.M. Jovanovic, Glassy carbon electrodes: I. Characterization and electrochemical activation, *Carbon* 39 (2001) 1195.
- [4] B.R. Kozub, N.V. Rees, R.G. Compton, Electrochemical determination of nitrite at a bare glassy carbon electrode; why chemically modify electrodes? *Sensors and Actuators B* 143 (2010) 539.
- [5] T.M. Florence, Anodic stripping voltammetry with a glassy carbon electrode mercury-plated in situ, *Journal of Electroanalytical Chemistry* 27 (1970) 273.
- [6] E. Fischer, C.M.G. van den Berg, Anodic stripping voltammetry of lead and cadmium using a mercury film electrode and thiocyanate, *Analytica Chimica Acta* 385 (1999) 273.
- [7] J. Wang, J. Lu, S.B. Hocevar, P.A.M. Farias, B. Ogorevc, Bismuth-coated carbon electrodes for anodic stripping voltammetry, *Analytical Chemistry* 72 (2000) 3218.
- [8] S.B. Hocevar, B. Ogorevc, J. Wang, B. Pihlar, A study on operational parameters for advanced use of bismuth film electrode in anodic stripping voltammetry, *Electroanalysis* 14 (2002) 1707.
- [9] A. Krolicka, R. Pauliuikaitė, I. Svancara, R. Metelka, A. Bobrowski, E. Norkus, K. Kalcher, K. Vytras, Bismuth-film-plated carbon paste electrodes, *Electrochemistry Communications* 4 (2002) 193.
- [10] E.A. Hutton, B. Ogorevc, S.B. Hocevar, M.R. Smyth, Bismuth film microelectrode for direct voltammetric measurement of trace cobalt and nickel in some simulated and real body fluid samples, *Analytica Chimica Acta* 557 (2006) 57.
- [11] C. Kokkinos, A. Economou, I. Raptis, C.E. Efstratiou, T. Speliotis, Novel disposable bismuth-sputtered electrodes for the determination of trace metals by stripping voltammetry, *Electrochemistry Communications* 9 (2007) 2795.
- [12] M. Frena, I. Campestrini, O.C. de Braga, A. Spinelli, In situ bismuth-film electrode for square-wave anodic stripping voltammetric determination of tin in biodiesel, *Electrochimica Acta* 56 (2011) 4678.
- [13] E.A. Hutton, B. Ogorevc, S.B. Hocevar, F. Weldon, M.R. Smyth, J. Wang, An introduction to bismuth film electrode for use in cathodic electrochemical detection, *Electrochemistry Communications* 3 (2001) 707.

- [14] D. Du, X.P. Ye, J.D. Zhang, D.L. Liu, Cathodic electrochemical analysis of methyl paration at bismuth modified glassy carbon electrode, *Electrochimica Acta* 53 (2008) 4478.
- [15] S.B. Hocevar, I. Svancara, B. Ogorevc, K. Vytras, Antimony film electrode for electrochemical stripping analysis, *Analytical Chemistry* 79 (2007) 8639.
- [16] E. Tesarova, L. Baldrianova, S.B. Hocevar, I. Svancara, K. Vytras, B. Ogorevc, Anodic stripping voltammetric measurement of trace heavy metals at antimony film carbon paste electrode, *Electrochimica Acta* 54 (2009) 1506.
- [17] K.E. Toghill, L. Xiao, G.G. Wildgoose, R.G. Compton, Electroanalytical determination of cadmium(II) and lead(II) using an antimony nanoparticle modified boron-doped diamond electrode, *Electroanalysis* 21 (2009) 1113.
- [18] C. Kokkinos, A. Economou, I. Raptis, T. Speliotis, Novel disposable microfabricated antimony-film electrodes for adsorptive stripping analysis of trace Ni(II), *Electrochemistry Communications* 11 (2009) 250.
- [19] V. Urbanova, K. Vytras, A. Kuhn, Macroporous antimony film electrodes for stripping analysis of trace heavy metals, *Electrochemistry Communications* 12 (2010) 114.
- [20] V. Guzsvany, H. Nakajima, N. Soh, K. Nakano, T. Imato, Antimony-film electrode for the determination of trace metals by sequential-injection analysis/anodic stripping voltammetry, *Analytica Chimica Acta* 658 (2010) 12.
- [21] B. Nigovic, S.B. Hocevar, Antimony film electrode for direct cathodic measurement of sulfasalazine, *Electrochimica Acta* 58 (2011) 523.
- [22] H. Sophie, V. Jovanowski, S.B. Hocevar, B. Ogorevc, In-situ plated antimony film electrode for adsorptive cathodic stripping voltammetric measurement of trace nickel, *Electrochemistry Communications* 20 (2012) 23.
- [23] V. Mirceski, S.B. Hocevar, B. Ogorevc, R. Gulaboski, I. Drangov, Diagnostics of anodic stripping mechanisms under square-wave voltammetry conditions using bismuth film substrates, *Analytical Chemistry* 84 (2012) 4429.
- [24] M. Lovric, Square-wave voltammetry, in: F. Scholz (Ed.), *Electroanalytical Methods: Guide to Experiments and Applications*, Springer-Verlag, Berlin, 2002, p. 111.
- [25] V. Mirceski, S. Komorsky-Lovric, M. Lovric, *Square-wave voltammetry: theory and applications*, in: F. Scholz (Ed.), *Monographs in Electrochemistry*, Springer, Heidelberg, 2007.
- [26] V. Mirceski, M. Lovric, Split square-wave voltammograms of surface redox reactions, *Electroanalysis* 9 (1997) 1283.
- [27] V. Mirceski, M. Lovric, Square-wave voltammetry of a cathodic stripping reaction complicated by adsorption of the reacting ligand, *Analytica Chimica Acta* 386 (1999) 47.
- [28] G. Kefala, A. Economou, A. Voulgaropoulos, M. Sofoniou, A study of bismuth-film electrodes for the detection of trace metals by anodic stripping voltammetry and their application to the determination of Pb and Zn in tap-water and human hair, *Talanta* 61 (2003) 603.